

Shape Model of the Maxillary Dental Arch using Fourier Descriptors with an Application in the Rehabilitation for Edentulous Patient

Omar M. Rijal, *Member, IEEE*, Norli A. Abdullah, Zakiah M. Isa,
Norliza M. Noor, *Senior Member, IEEE*, Omar F. Tawfiq

Abstract—The knowledge of teeth positions on the maxillary arch is useful in the rehabilitation of the edentulous patient. A combination of angular (θ), and linear (l) variables representing position of four teeth were initially proposed as the shape descriptor of the maxillary dental arch. Three categories of shape were established, each having a multivariate normal distribution. It may be argued that 4 selected teeth on the standardized digital images of the dental casts could be considered as insufficient with respect to representing shape. However, increasing the number of points would create problems with dimensions and proof of existence of the multivariate normal distribution is extremely difficult. This study investigates the ability of Fourier descriptors (FD) using all maxillary teeth to find alternative shape models. Eight FD terms were sufficient to represent 21 points on the arch. Using these 8 FD terms as an alternative shape descriptor, three categories of shape were verified, each category having the complex normal distribution.

I. INTRODUCTION

There is a steady trend in modeling the maxillary dental arch shape [1,2,3]. Determination of the arch shape has many clinical applications such as in maxillofacial surgery, orthodontic, prosthetic treatment and forensic dentistry [2,4,5]. In the rehabilitation of edentulism, one of the most important achievements of the dental prosthesis is to fulfil a natural and younger appearance to the patient and aesthetics by providing proper support to the soft tissue. This makes a constant challenge to the dentists as the anterior upper teeth should be positioned as close as possible to the positions originally occupied by the natural teeth [6].

*Research supported by the Institute of Research Management and Monitoring (IPPP), University of Malaya and Ministry of Higher Education (MOHE) under SLAI program.

O. M. Rijal is with the Institute of Mathematical Sciences, Faculty of Science, University of Malaya, Kuala Lumpur, Malaysia (corresponding author tel.: +6019-3304072; fax: +603-7967-4143; e-mail: omarrija@um.edu.my).

N. A. Abdullah is a PhD student of the Institute of Mathematical Sciences, Faculty of Science, University of Malaya, Kuala Lumpur, Malaysia (e-mail: norlienih@yahoo.com).

Z. M. Isa is with Department of Prosthetic Dentistry, Faculty of Dentistry, University of Malaya, Kuala Lumpur, Malaysia (e-mail: zakiah@um.edu.my).

N. M. Noor is with the Department of Engineering, UTM Razak School of Engineering and Advanced Technology, Universiti Teknologi Malaysia, Malaysia (e-mail: norliza@ic.utm.my).

O. T. Farouq is a PhD student of the Department of Prosthetic Dentistry, Faculty of Dentistry, University of Malaya, Kuala Lumpur, Malaysia (e-mail: dromar_s@yahoo.com).

In a pilot study [7, 8], three common landmarks was used to establish the Cartesian coordinate system to represent points on the maxillary arch. Four points (θ_{iw}, l_{iw}), $w = 1, \dots, 4$ from four teeth were selected and the shape descriptor $v_i = (\theta_{i1}, l_{i1}, \theta_{i2}, l_{i2}, \theta_{i3}, l_{i3}, \theta_{i4}, l_{i4})$, $i = 1, \dots, 47$ represented the shape of 47 dental casts. Three categories of shapes were derived using v and each category has a unique multivariate normal distributions (MVN). However, v as derived from four teeth has limited application in prosthetic dentistry. In the rehabilitation of the edentulous patient (patient who has lost all his teeth), the knowledge of a complete set of teeth is required. The curse of dimensionality would arise if the number of variables in v is increased, and formally proving the MVN as the shape model is extremely difficult.

This study using the same data set as in the pilot study [7,8] investigates the suitability of the Fourier descriptor (FD) as a shape descriptor for the dental arch. To avoid the curse of dimensionality, a relatively small number of FD terms is sought after to enable the formulation of a new shape model.

The knowledge of teeth positions and the categories of arch shape has great potential in achieving aesthetic values and functional properties when rehabilitating the edentulous patient.

II. MATERIALS AND METHOD

A. Alignment of Images

For every image of the dental cast (Fig. 1), three landmarks defined a Cartesian coordinate system. The line passing through the two hamular notches define the x-axis. The line vertical to the x-axis and passing through the incisive papilla define the y-axis. The intersection of these lines define the origin. Two rulers in the image allow distances in terms of the number of pixels to be converted to millimeters.

Each dental cast was represented by twenty-one corresponding points. These points are made up of the cusps tips of 18 maxillary teeth, the two hamular notches and the origin.

B. Fourier Descriptor

Forty seven standardized digital images of dental casts were considered in this study. The 21 points representing the dental arch shape were rearranged in an anti-clockwise sequence starting from the origin and denoted as

$[x(0), y(0)], [x(1), y(1)], \dots, [x(N-1), y(N-1)]$, (Fig. 1). Each coordinate pair can be treated as a complex number so that $s(k) = x(k) + jy(k)$, where $k = 0, 1, \dots, N-1$ and $N = 21$.

The discrete Fourier transform (DFT) of $s(k)$ is

$$a_u = \frac{1}{N} \sum_{k=0}^{N-1} s(k) \exp\left(-\frac{j2\pi uk}{N}\right) \quad (1)$$

for $u = 0, 1, \dots, N-1$, [9]. The complex coefficients a_u are known as the Fourier descriptors (FD) of the boundary. The set of FD for each dental arch was denoted as $\mathbf{A}_i = [a_0^i, a_1^i, \dots, a_{N-1}^i]$, $i = 1, \dots, 47$ where

$$a_u^i = c_u^i + jd_u^i. \quad (2)$$

The inverse Fourier transform of these coefficients restores $s(k)$, as given by,

$$s(k) = \sum_{u=0}^{N-1} a_u \exp\left(\frac{j2\pi uk}{N}\right) \quad (3)$$

for $k = 0, 1, \dots, N-1$.

An approximation of the shape boundary can be obtained by judiciously selecting q - a_u terms where $q < N$. When q - a_u terms are used, the estimate of \mathbf{A}_i is denoted as $\hat{\mathbf{A}}_i$.

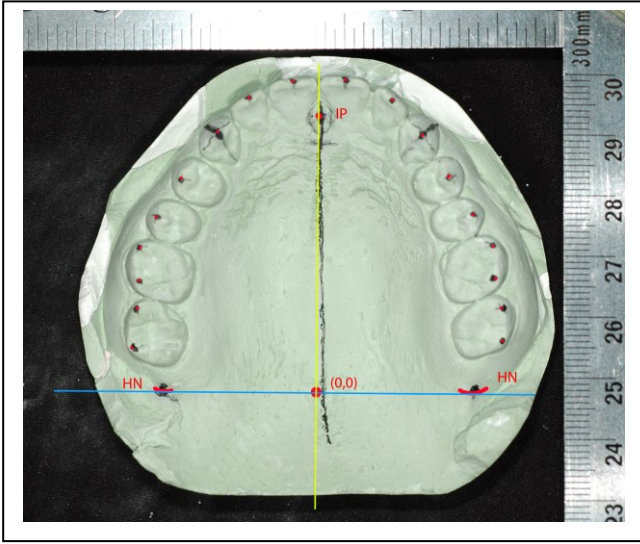


Figure 1: The hamular notches (HN) and the incisive papilla (IP) were used to establish the Cartesian coordinate. 21 selected points were illustrated in the diagram.

C. Selecting the number of FD terms (q)

The q largest a_u values were selected and re-substituted in Equation (3), whilst the remaining a_u terms were ignored [10]. The 21 points, \mathbf{x}_r^o , $r = 1, \dots, 21$, obtained by using these

q - a_u terms and $q < N$, have to be compared with the corresponding 21 points, \mathbf{x}_r^m , $r = 1, \dots, 21$, when all a_u terms were considered. A measure of similarity between these two shapes will show the appropriateness of the choice of q .

Since the images are aligned, the Procrustes distance

$$PD_i = \sum_{r=1}^N (\mathbf{x}_r^o - \mathbf{x}_r^m)' (\mathbf{x}_r^o - \mathbf{x}_r^m) \quad (4)$$

can be used as a similarity measure [11, 12]. The value of q that minimizes PD_i will be regarded as the optimal choice of q .

D. Nearest Neighbor Discrimination

The pilot study [7, 8] showed three categories of shape which in this study may be represented by $\hat{\mathbf{A}}_i = [\hat{a}_1^i, \hat{a}_2^i, \dots, \hat{a}_q^i]$, where $i = 1, \dots, 11$ for the first category, $i = 12, \dots, 34$ for the second category, and $i = 35, \dots, 49$ for the third category, with $\bar{\hat{\mathbf{A}}}^g$ ($g = 1, 2, 3$) as the respective means. The nearest neighbor method is then used to verify the existence of the three categories of shape.

Without loss of generality, the number of $\hat{\mathbf{A}}_i$, $i = 1, \dots, 11$, which is not closest to $\bar{\hat{\mathbf{A}}}^1$ will enable the estimation of the misclassification probability for the first shape category. Table II gives the misclassification probability using the Procrustes distance and Table III gives the misclassification probability for the Hausdorff distance [13].

E. Probability Distribution of $\hat{\mathbf{A}}$

Let $\hat{\mathbf{A}}_i = \hat{\mathbf{c}}_i + j\hat{\mathbf{d}}_i$ where $\hat{\mathbf{c}}_i^T = (\hat{c}_1^i, \hat{c}_2^i, \dots, \hat{c}_q^i)$ and $\hat{\mathbf{d}}_i^T = (\hat{d}_1^i, \hat{d}_2^i, \dots, \hat{d}_q^i)$ (see Equation(2)). The Kolmogorov - Smirnov test investigated univariate normality of the components of $\hat{\mathbf{c}}^T$ and $\hat{\mathbf{d}}^T$, [14]. If all components are univariate normal then $\hat{\mathbf{c}}^T$ and $\hat{\mathbf{d}}^T$ are MVN vectors. Further $\hat{\mathbf{c}} + j\hat{\mathbf{d}}$ will then have the complex normal distribution [15, 16, 17].

III. RESULTS AND DISCUSSION

The ability of the 8 FD terms to represent the 21 points of the teeth position is illustrated in Table I. The Procrustes distance decreases rapidly when q changes from 2 to 8 and gradually levels off for increasing q . The 8-FD terms used

were $\hat{A}_i = (\hat{a}_1^i, \hat{a}_2^i, \hat{a}_3^i, \hat{a}_4^i, \hat{a}_5^i, \hat{a}_6^i, \hat{a}_{20}^i, \hat{a}_{21}^i)$ where $\hat{a}_u^i = \hat{c}_u^i + j\hat{d}_u^i$. Fig. 2 illustrates one case of the original 21 points of the dental arch overlaid with the 21 points derived from the 8-FD terms.

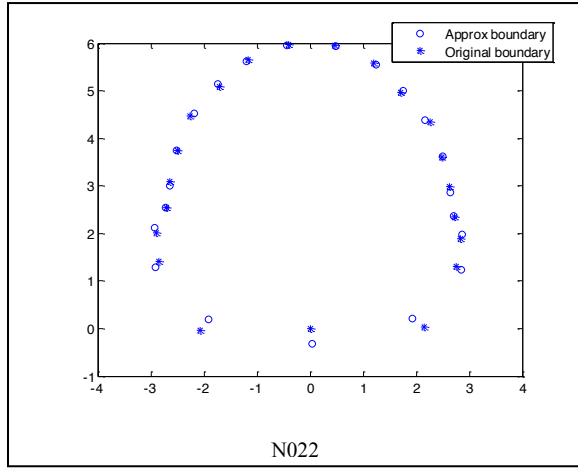


Figure 2: Comparison of arch shape for case N022 when using all FD terms (original boundary) relative to using 8-FD terms (approximate boundary).

This result enables the definition of mean shape using 8-FD terms, in particular, let,

$$\bar{\hat{A}}^1 = (2.9753 + 63.5671i, -1.6451 - 59.4081i, -0.1445 - 7.7225i, -0.1546 - 9.4307i, 0.0583 - 4.5459i, 0.1717 - 2.6657i, -0.0124 + 5.8928i, 0.1148 + 4.5777i)$$

$$\bar{\hat{A}}^2 = (-0.6514 + 57.6496i, -0.4808 - 57.5987i, 0.0425 - 7.2191i, 0.0374 - 8.3538i, 0.0037 - 4.2743i, 0.0793 - 2.4500i, 0.0559 + 6.7442i, 0.0980 + 5.5652i)$$

and

$$\bar{\hat{A}}^3 = (3.1967 + 3.6151i, 1.2862 + 2.0317i, 0.2656 + 1.2674i, 0.2737 + 0.5634i, 0.2404 + 0.7673i, 0.2770 + 0.3759i)$$

The nearest neighbor discrimination method using these three means, $\bar{\hat{A}}^g$ ($g = 1, 2, 3$), showed relatively small misclassification probabilities when using the Procrustes distance (Table II) and the Hausdorff distance (Table III) except for the discrimination of Group C from $\bar{\hat{A}}^1$. These results support the existence of three categories of shape.

For completeness, variation of shape must be stated and this is done by seeking the probability distribution of the \hat{A}_i . Table IV strongly suggests that \mathbf{c} has a multivariate normal distribution (MVN) when making use of the Kolmogorov-Smirnov test for normality, [14]. Similarly, Table V strongly suggests that \mathbf{d} also has a MVN probability distribution.

Since $\hat{A}_i = \hat{\mathbf{c}}_i + j\hat{\mathbf{d}}_i$ where $\hat{\mathbf{c}}_i^T = (\hat{c}_1^i, \hat{c}_2^i, \hat{c}_3^i, \hat{c}_4^i, \hat{c}_5^i, \hat{c}_6^i, \hat{c}_{20}^i, \hat{c}_{21}^i)$ and $\hat{\mathbf{d}}_i^T = (\hat{d}_1^i, \hat{d}_2^i, \hat{d}_3^i, \hat{d}_4^i, \hat{d}_5^i, \hat{d}_6^i, \hat{d}_{20}^i, \hat{d}_{21}^i)$, therefore \hat{A}_i has the well-known [15,16,17] complex multi-normal probability

distribution $CN(\boldsymbol{\mu}, \Gamma, C)$ which can be described with three parameters,

$$\boldsymbol{\mu} = E(\hat{A}_i), \quad (5)$$

$$\Gamma = E[(\hat{A}_i - \boldsymbol{\mu})(\hat{A}_i^* - \boldsymbol{\mu}^*)^T], \quad (6)$$

$$C = E[(\hat{A}_i - \boldsymbol{\mu})(\hat{A}_i - \boldsymbol{\mu})^T] \quad (7)$$

where \hat{A}_i^T denotes matrix transpose and \hat{A}_i^* denotes complex conjugate. However, more data are required before estimation and hypotheses testing issues can be addressed.

TABLE I. THE PROCTUSTES DISTANCES BETWEEN THE ORIGINAL 21 POINTS AND THEIR ESTIMATED POSITIONS USING m -FD TERMS

q \ Cast	N022	N006
2	10.7183	11.7878
3	9.6296	9.7249
4	6.9755	7.1635
5	6.0497	5.8353
6	4.7509	4.5743
7	3.7702	3.6664
8	2.6487	2.9457
9	2.0986	2.3607
10	2.0861	2.3897
11	1.8344	2.1844
12	1.6422	1.8541
13	1.6041	1.5330
14	1.3952	1.2555
15	1.2179	1.1104
16	0.9375	0.8857
17	0.8061	0.7930
18	0.6438	0.6230
19	0.5019	0.4312
20	0.3318	0.2648
21	3.7942e-014	2.2862e-014

TABLE II. THE MISCLASSIFICATION PROBABILITY FOR NEAREST NEIGHBOUR USING PROCRUSTES DISTANCE

Dental cast group	$\bar{\hat{A}}^1$	$\bar{\hat{A}}^2$	$\bar{\hat{A}}^3$
Group A	0	0.0909	0.2727
Group B	0.0909	0	0.0909
Group C	0.2857	0.0714	0

TABLE III. THE MISCLASSIFICATION PROBABILITY FOR NEAREST NEIGHBOUR USING HAUSDORFF DISTANCE

Dental cast group	\hat{A}^1	\hat{A}^2	\hat{A}^3
Group A	0	0.1818	0.0909
Group B	0.0909	0	0.0454
Group C	0.2857	0.0714	0

TABLE IV. KOLMOGOROV-SMIRNOV TEST STATISTICS AND CRITICAL VALUE (CV) FOR $\hat{c}_1, \hat{c}_2, \hat{c}_3, \hat{c}_4, \hat{c}_5, \hat{c}_6, \hat{c}_{20}$ AND \hat{c}_{21}

Real part variable FD	Group 1 CV=0.3912	Group 2 CV=0.2809	Group 3 CV=0.3489
c_1	0.1375	0.1289	0.0894
c_2	0.1799	0.1422	0.1814
c_3	0.1460	0.1486	0.1057
c_4	0.2378	0.1443	0.1238
c_5	0.2719	0.1579	0.1733
c_6	0.1280	0.1253	0.1619
c_{20}	0.2050	0.1554	0.1260
c_{21}	0.1323	0.1340	0.1957

TABLE V. KOLMOGOROV-SMIRNOV TEST STATISTICS AND CRITICAL VALUE (CV) FOR $\hat{d}_1, \hat{d}_2, \hat{d}_3, \hat{d}_4, \hat{d}_5, \hat{d}_6, \hat{d}_{20}$ AND \hat{d}_{21}

Imaginary part variable FD	Group 1 CV=0.3912	Group 2 CV=0.2809	Group 3 CV=0.3489
d_1	0.1600	0.1124	0.1212
d_2	0.2188	0.1388	0.1244
d_3	0.1671	0.0937	0.1657
d_4	0.1518	0.1394	0.2379
d_5	0.1673	0.1012	0.1360
d_6	0.2268	0.1131	0.1721
d_{20}	0.1142	0.1380	0.0896
d_{21}	0.2140	0.1075	0.1497

IV. CONCLUSION

The use of $CN(\mu, \Gamma, C)$ as a shape model will give the precise locations of the 18 teeth on the maxillary arch and will be useful for applications in rehabilitating edentulous patients. In particular, this will help the dentist to position the upper anterior teeth as close as possible to the position originally occupied by the natural teeth. This in turn makes it possible to achieve a natural and younger appearance to the patient and aesthetics by providing proper support to the soft tissue.

REFERENCES

[1] M. J. Felton, P. M. Sinclair, D. L. Jones, R.G. Alexander. A computerized analysis of the shape and stability of Mandibular arch form. *Am J Orthod Dentofacial Orthop* 1987: 92; 478-83.

[2] M. Raberin, B. Lai, J. L. Martom, F. Brunner, Dimensions and form of dental arches in subjects with normal occlusions, *American journal of orthodontics and dentofacial orthopedics* 104, pp. 67-72, 1993.

[3] V F Ferrario, C Sforza, C Dellavia, A Colombo, R P Ferrari. Three-dimensional hard tissue palatal size and shape: A 10-year longitudinal evaluation in healthy adults. *Int J Adult Orthod Orthognath Surg* 17(1): 51-8, 2002.

[4] G. Preti, P. Pera, and F. Bassi, Prediction of the shape and size of the maxillary anterior arch in edentulous patients, *Journal of Oral Rehabilitation* 13 (1986), pp. 115-125.

[5] M.A. Bush, P.J. Bush, and H.D. Sheets, Similarity and match rates of the human dentition in three dimensions: relevance to bitemark analysis, *International Journal of Legal Medicine* 125 (2011), pp. 779-784.

[6] P.S. Fu, C.C. Hung, J. M. Hong, J. C. Wang, C. F. Tsai, Y. M. Wu, Three-dimensional relationship of the maxillary anterior teeth to the incisive papilla in young adults. *Kaohsiung J Med Sci.* 2007 Oct; 23(10):519-525.

[7] O. M. Rijal, N. A. Abdullah, Z. M. Isa, F. A. Davaei, N. M. Noor, O. F. Tawfiq "A Novel Shape Representation of the Dental Arch and its Applications in Some Dentistry Problems," In *Proc. 33rd Annual International Conference of the IEEE EMBS*, Boston, 2011, pp. 5092-5095.

[8] O. M. Rijal, N. A. Abdullah, Z. M. Isa, N. M. Noor, O. F. Tawfiq "A Probability Distribution of Shape for the Dental Maxillary" In *Proc. 34th Annual International Conference of the IEEE EMBS*, San Diego, 2012, pp. 5420-5423

[9] A. V. Oppenheim, A. S. Willsky, I. T. Young. *Signals and Systems*. New Jersey: Prentice-Hall, 1983.

[10] L. F. D. Costa, R. M. Cesar Jr. *Shape analysis and classification: theory and practice*. Florida: CRC Press, Inc, 2000.

[11] D. Zhang, and G. Lu, A comparative study on shape retrieval using Fourier descriptors with different shape signatures, in *Proceedings of international conference on intelligent multimedia and distance education (ICIMADE01)*, Fargo, USA, 2001, pp. 1-9.

[12] K. V. Mardia, J. T. Kent, J. M. Bibby. *Multivariate Analysis*, London: Academic Press, 1979.

[13] D. P. Huttenlocher, G. A. Klanderman, and W. J. Rucklidge, Comparing images using the Hausdorff distance, *IEEE Trans. PAMI*, vol. 15, pp. 850-863, 1993.

[14] E. J. Dudewicz, S. N. Mishra, *Modern Mathematical Statistics*, Singapore: Wiley, 1988, pp. 670.

[15] R. A. Wooding, The multivariate distribution of complex normal variables, *Biometrika*, 43, pp.329-350, 1956.

[16] N. R. Goodman, Statistical analysis based on a certain multivariate complex Gaussian distribution (An Introduction). *Ann. Math. Statist.* 34, pp.152-177, 1963.

[17] C. G. Khatri, Classical statistical analysis based on a certain multivariate complex Gaussian distribution. *Ann. Math. Statist.* 36, pp.98-114, 1965.